Anomalous Properties of Poly(methyl methacrylate) Thin Films in Supercritical Carbon Dioxide

S. M. Sirard, K. J. Ziegler, I. C. Sanchez, P. F. Green,* and K. P. Johnston*

Department of Chemical Engineering, The University of Texas at Austin, Austin, Texas 78712

Received August 2, 2001

ABSTRACT: Carbon dioxide produces an anomalous maximum in the swelling of poly(methyl methacrylate) (PMMA) thin films that is not present in bulk films, as shown with in-situ spectroscopic ellipsometry. This maximum and a corresponding minimum in refractive index are observed in regions of pressure where CO_2 is highly compressible near the critical point. An effective excess thickness, determined from the height of the anomalous swelling maxima, increases proportionally with increasing initial film thickness, h_0, in the range studied of 85 nm < h_0 < 325 nm. Therefore, the anomalous swelling maxima suggest concentration inhomogeneities in the thin film, i.e., the onset of polymer/CO_2 phase separation, that are influenced by the compressibility of the system and the confinement of the film. The PMMA swelling isotherms are insensitive to changing the substrate from silicon to gallium arsenide.

Introduction

Liquid and supercritical carbon dioxide (CO_2) have emerged as leading alternatives to toxic organic solvents in polymer processing and synthesis.[1] Carbon dioxide is abundant, nontoxic, and inflammable. In addition, large changes in the density of supercritical CO_2 can be achieved with small variations in pressure and/or temperature, resulting in the ability to tune the solvent quality. The unique properties of CO_2 have been used advantageously in the modification of polymeric films, through extraction and impregnations,[1,2] foaming of polymer films,[3] coating[4] and development of photoresist films in lithography,[5] and in the formation of polymer−metal nanocomposites.[6] Supercritical CO_2 has also been used as a drying agent for photoresist films so as to prevent the deformation and collapse of high-aspect-ratio resist lines by minimizing the capillary forces during drying.[7]

The tunable properties of compressed CO_2 make it an attractive candidate for manipulating and controlling surface properties of polymer thin films. Studies with Monte Carlo simulation and lattice fluid self-consistent-field theory indicate that the large compressibility of a supercritical fluid influences the swelling of polymer thin films and the intermolecular forces between surfaces with adsorbed and grafted polymer layers.[8,9] In-situ studies of thin films exposed to high-pressure CO_2 are scarce due to experimental challenges. Previous studies have examined adsorption of CO_2 on nonswelling hard surfaces. Findenegg[10] showed large surface excesses of ethylene on homogeneous graphitized carbon black surfaces near the critical pressure and critical temperature. In addition, similar excesses of CO_2 have been observed experimentally on both modified and unmodified silica hard surfaces.[11−13] The critical adsorption phenomena have also been successfully modeled.[14]

Recently, we demonstrated that spectroscopic ellipsometry is a useful probe for analyzing thin films exposed to high-pressure fluids.[13] The swelling of poly(dimethylsiloxane) (PDMS) thin films by CO_2 was slightly greater than the swelling measured for bulk PDMS.[13] In ellipsometry, the resultant change in the polarization of light reflected from a film is used to determine the thickness and refractive index of the film. At atmospheric pressure, spectroscopic ellipsometry has been used to study many polymer thin film phenomena including glass transition temperatures,[15] adsorption of polymers and surfactants,[16] and swelling of thin films.[13,17]

The primary objective of this study is to examine the swelling of supported poly(methyl methacrylate) (PMMA) thin films, with emphasis in regions where CO_2 is highly compressible. Our hypothesis from the above theoretical studies[8] is that the large compressibility of CO_2 will produce unusual behavior in the swelling of soft penetrable surfaces. Because CO_2 penetrates the thin film, the behavior may be expected to be quite different than observed previously for hard surfaces. In an attempt to develop a mechanistic explanation of thin film swelling by CO_2, the initial film thickness is varied from 85 to 325 nm. Spectroscopic ellipsometry is used to determine simultaneously the thickness and refractive index of these swollen un-cross-linked PMMA films. In addition, the effects of interactions with the substrate are probed by comparing swelling isotherms of PMMA coated on both gallium arsenide (GaAs) and a more hydrophilic silicon dioxide (SiO_2). A secondary objective is to examine how CO_2 influences the glass transition of PMMA thin films.

Experimental Section

Materials. PMMA (MW = 224 000, M_w/M_n = 1.04) was purchased from Polysciences Inc. Initially, the PMMA was dissolved in toluene (EM Science). The PMMA/toluene solution was spin-coated onto both silicon (100) and GaAs (100) wafers.

Sample Preparation. The wafers were cut into 1 × 1 cm squares and were initially cleaned[18] by soaking in a 50:50 (w/w) hydrochloric acid (EM Science)/methanol (EM Science) solution for 30 min. The wafers were then rinsed with voluminous amounts of deionized water (NANOpureII, Barnstead) and then dried with nitrogen gas (Matheson Gas Products, >99.999%). The wafers were then soaked in 95% sulfuric acid (Mallinckrodt, analytical grade) for 30 min and subsequently were rinsed with deionized water and dried with nitrogen gas.

The native oxide thickness was measured with spectroscopic ellipsometry prior to coating the silicon wafers and was found

* Corresponding authors: email: green@che.utexas.edu; kpj@che.utexas.edu.

10.1021/ma011384w CCC: $22.00
Published on Web 02/01/2002

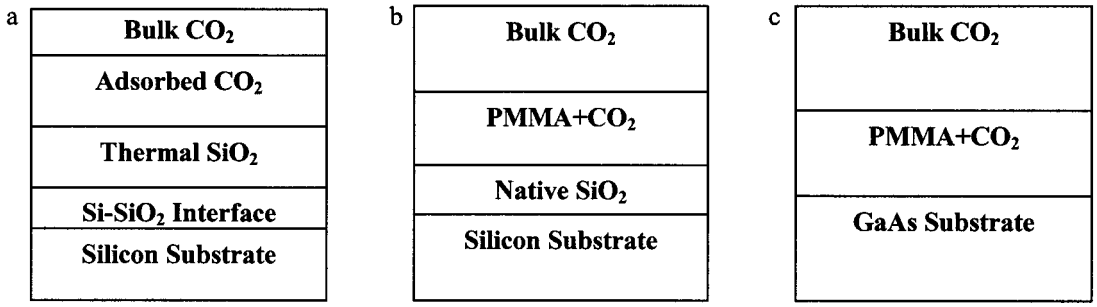

Figure 1. (a) Five-layer model for fitting the thickness of an adsorbed CO_2 layer on a bare thermal SiO_2. (b) Four-layer model used for fitting the thickness and refractive index of swollen PMMA films on the native oxide of a silicon wafer. (c) Three-layer model for fitting the thickness and refractive index of swollen PMMA films on GaAs.

to be between 1.5 and 2.5 nm in all of the experiments. The films were spun onto the wafers using a photoresist spinner (Headway Research, Inc.). The concentration of the PMMA/toluene solution and the spin rate were varied to obtain films of the desired thickness. The coated wafers were annealed under vacuum at 170 °C for 66 h to remove any residual solvent and to relax any spin-coating-induced strains.

Ellipsometry. A M-44 spectroscopic ellipsometer set up in the rotating analyzer configuration (J.A. Woollam Co., Inc.) was used for all of the experiments. The angle of incidence for all measurements was 70° from the vertical. The experiments were performed in a high-pressure ellipsometry cell using fused silica windows (Almaz Optics). The details of the cell design can be found elsewhere.[13] A couple of modifications were made to the cell. Kalrez O-rings (Southwest Seal & Supply Co.) were used to seal the windows and caps instead of epoxy. In addition, a torque wrench was used to consistently put an equivalent and minimal amount of torque needed to seal the windows. We found that these changes reduce the amount of window birefringence markedly.

Once a sample was loaded into the cell, CO_2 (Air Products, >99.9999%) was charged to the cell using a manual pressure generator (High-Pressure Equipment Co.). Pressure was controlled with a strain gauge pressure transducer (Sensotec). The pressure transducer was calibrated to within ±1 psi. Typically, 10−20 min was allowed for equilibration of the swollen thin films between pressure changes. The cell was heated using four cartridge heaters (Omega) that were inserted at the top of the cell. Temperature was controlled with a PID temperature controller (Omega) that was calibrated prior to the experiments. The cell was allowed to reach thermal equilibrium for at least 60 min at each temperature.

Thermal Oxide Measurements. A five-layer model, as shown in Figure 1a, was used to fit the data taken on the thermal oxide wafer (i.e., an oxide layer that is grown at high temperatures). The refractive indexes of the thermal oxide, Si−SiO_2 interface layer, and the silicon substrate layer were fixed from literature values.[19] Justification for using this model is given elsewhere.[19] In addition, the refractive index of the CO_2 atmosphere layer at each pressure and temperature was fixed from literature values.[20] The thickness of the adsorbed CO_2 layer was fit for assuming the refractive index of a hypothetical liquid at the same temperature ($n = 1.23$).

Swelling Experiments. A four-layer model, as shown in Figure 1b, was used to fit the swelling data for the PMMA films supported on silicon. The model contains a bulk CO_2 atmosphere layer, a swollen polymer layer, a native oxide layer, and a silicon substrate layer. Literature values were used for the refractive index of the native oxide,[21] silicon substrate,[22] and CO_2[20,23] layers. The fitting parameters in the swelling experiments were the thickness and refractive index of the swollen polymer film, the angle of incidence, and the offset in the ellipsometric delta parameter due to window birefringence. The refractive index of the polymer film was modeled using a Cauchy dispersion relationship[24]

$$n(\lambda) = A + \frac{B}{\lambda^2} + ... \qquad (1)$$

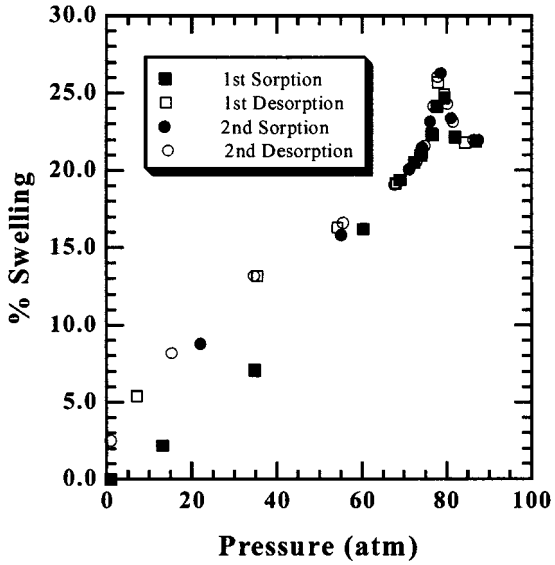

Figure 2. Swelling isotherm for PMMA thin film coated on GaAs wafer. Squares (■, □) represent the first sorption/desorption runs, and circles (●, ○) represent the second sorption/desorption runs. Filled squares/circles represent sorption runs, and open squares/circles represent desorption runs.

For the PMMA films supported on GaAs, a three-layer model, shown in Figure 1c, was used to fit the swelling data. The GaAs wafers do not contain a stable oxide, so the native oxide layer was excluded from this model. The optical constants for bare GaAs were measured with spectroscopic ellipsometry prior to coating with the PMMA films. The fitting parameters for these swelling experiments were the same as described above for the PMMA films coated on silicon. In each case, the swelling was determined by the following equation, assuming uniaxial swelling

$$\frac{\Delta V}{V_0}(\%) = \frac{h - h_0}{h_0} \times 100\% \qquad (2)$$

where V_0 is the initial volume of the film, h is the thickness of the swollen film, and h_0 is the initial thickness of the PMMA films determined by spectroscopic ellipsometry at 0 psig.

Results

The swelling experiments were conducted by performing alternating sorption/desorption runs. Figure 2 displays a representative swelling isotherm for a PMMA film ($h_0 \sim 89$ nm) coated on GaAs, and Figure 3 shows the average refractive index over the wavelength range scanned of the CO_2-swollen PMMA. In all of the experiments, the data exhibited a hysteresis at pressures below 50−60 atm between the initial sorption run and the subsequent sorption/desorption runs. In each case

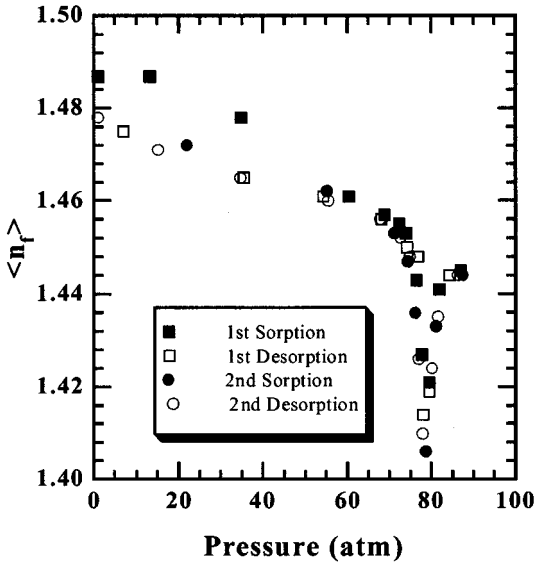

Figure 3. Average refractive indices of swollen PMMA thin film coated on GaAs wafer. Squares (■, □) represent the first sorption/desorption runs, and circles (●, ○) represent the second sorption/desorption runs. Filled squares/circles represent sorption runs, and open squares/circles represent desorption runs.

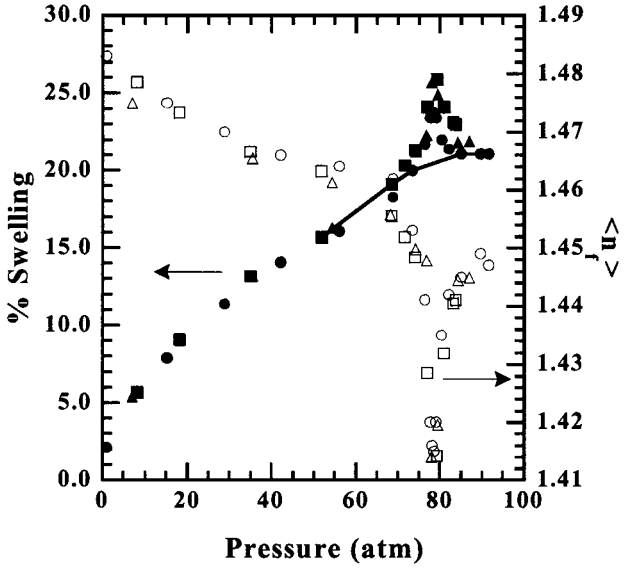

Figure 4. Swelling isotherms and average refractive indices of swollen PMMA thin films at 35 °C. Isotherms represent the first desorption runs. Filled symbols represent swelling isotherms, and corresponding open symbols represent refractive index isotherms. Circles (●, ○) represent $h_0 = 88$ nm on SiO_2, squares (■, □) represent $h_0 = 321$ nm on SiO_2, and triangles (▲, △) represent $h_0 = 89$ nm on GaAs. The solid line represents the interpolated baseline swelling.

the swelling values were larger during the first desorption cycle. Successive desorption runs approach a reproducible metastable state. The onset of the hysteresis in our swelling isotherms signifies the onset of the CO_2-induced glass transition. At CO_2 pressures higher than the glass transition pressure, the swelling is reversible when increasing or decreasing the pressure because the system is at equilibrium. At pressures below the glass transition pressure, the system exhibits hysteresis because the polymer is in a nonequilibrium state and the kinetics become controlling.

An anomalous maximum is observed in Figure 2 that corresponds to a sharp minimum in the refractive index of the swollen PMMA as seen in Figure 3. This maximum has not been seen in the swelling of bulk PMMA.[25,26] Furthermore, the isotherm is insensitive to changing the substrate to the more hydrophilic silica or to increasing the initial film thickness up to 320 nm, as seen in Figure 4. Similar behavior is seen in Figure 5 for the refractive index and swelling isotherms of two thin films of PMMA on silica ($h_0 = 85$ and 325 nm) at 50 °C.

The swelling isotherms in Figures 4 and 5 represent the first desorption cycles. The data at both temperatures show peculiar maxima in the swelling and corresponding minima in refractive indices that occur at different pressures for the different temperatures. At 35 °C, the maxima in swelling occur at a pressure slightly above the critical pressure. At 50 °C, the maxima in swelling and minima in refractive index are more subtle and broader than at 35 °C and occur at a higher pressure.

The swelling isotherms in Figures 4 and 5 can be plotted against CO_2 activity to produce a simpler representation of the data. Figures 6 and 7 show the swelling isotherms and the corresponding refractive indices plotted against CO_2 activity, respectively. At higher CO_2 activities, the isotherms at the two temperatures nearly fall on the same line since the system is at equilibrium and the volume fraction of CO_2 in the polymer does not change appreciably with temperature

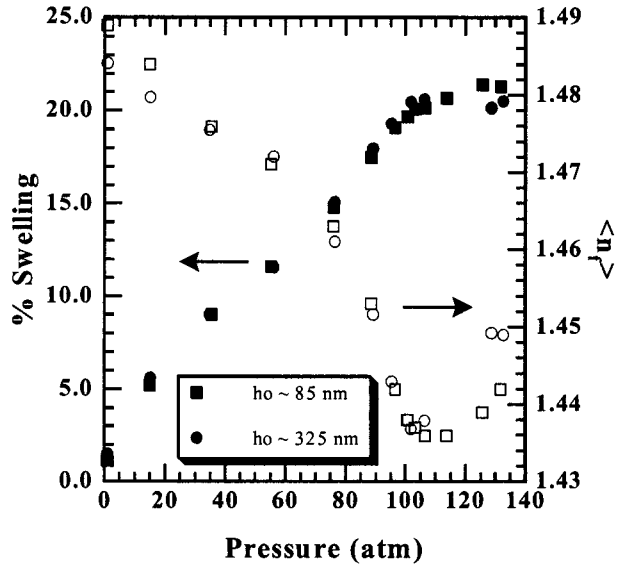

Figure 5. Swelling isotherms and average refractive indices of swollen PMMA thin films at 50 °C. Isotherms represent the first desorption runs. Filled symbols represent swelling isotherms, and corresponding open symbols represent refractive index isotherms. Squares (■, □) represent $h_0 = 85$ nm on SiO_2, and circles (●, ○) represent $h_0 = 325$ nm on SiO_2.

for a given value of activity. At these activities, the swelling isotherm curvature is upward, which is characteristic of the liquid state. At lower activities the isotherms at 35 °C are higher with respect to swelling and lower with respect to refractive index for a given activity compared with those at 50 °C. In addition, at these lower activities the curvature of the swelling isotherm is downward, which is characteristic of dual-mode sorption in the glassy state.

The ellipsometric measurements are sensitive enough to measure adsorption of CO_2 on a bare substrate. In Figure 8, the regressed thickness of the adsorbed CO_2 layer at 35 °C on a bare thermal oxide is shown

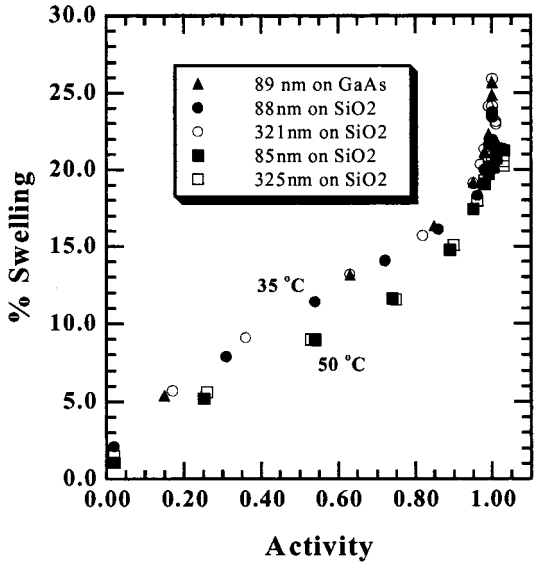

Figure 6. Swelling of PMMA films vs CO_2 activity. Isotherms represent first desorption runs. Triangle (▲) and circle (●, ○) symbols represent data at 35 °C, and squares represent data at 50 °C.

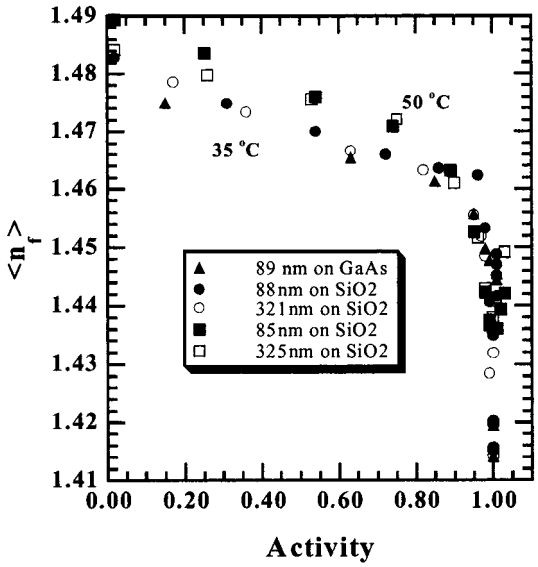

Figure 7. Average refractive indices of swollen PMMA films vs CO_2 activity. Isotherms represent first desorption runs. Triangle (▲) and circle (●, ○) symbols represent data at 35 °C, and squares (■, □) represent data at 50 °C.

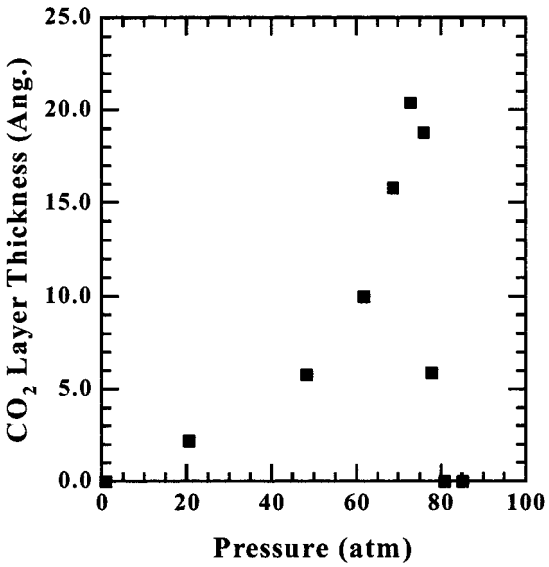

Figure 8. Adsorbed CO_2 layer thickness on thermally grown SiO_2.

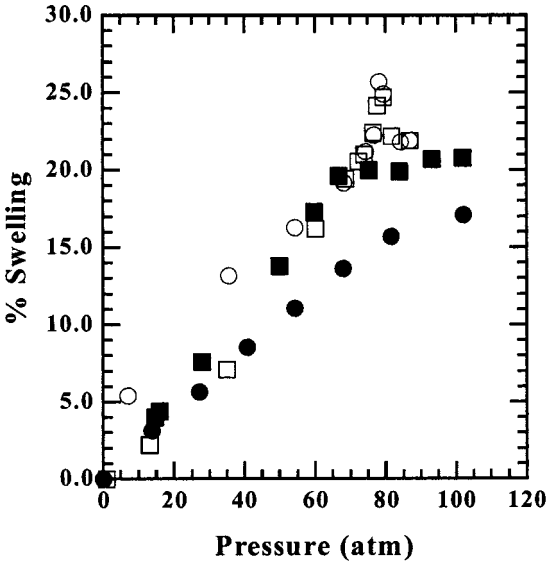

Figure 9. Comparison of swelling isotherms. Filled squares (■) are from ref 25. Filled circles (●) are from ref 26. Open circles (○) are the first desorption swelling isotherm of PMMA on GaAs from this study (h_0 = 89 nm). Open squares (□) are the first sorption swelling isotherm of PMMA on GaAs from this study.

assuming a refractive index of 1.23 (corresponding to pure hypothetical liquid CO_2 at 35 °C with a molar volume of ~46.6 mL/mol) for the adsorbed layer. We see a sharp maximum in the thickness of the adsorbed CO_2 layer near the critical pressure that reaches a thickness of approximately 2 nm.

Previous studies on the dilation of bulk PMMA films with CO_2 do not show maxima in the swelling isotherms.[25,26] However, it should be noted that many of the traditional techniques used to measure swelling/sorption in bulk films suffer from uncertainties in buoyancy corrections and equation of state calculations near the critical point. The swelling isotherms in Figure 2 are compared in Figure 9 with the data of Wissinger et al.[25] for the swelling of bulk PMMA with CO_2 at 32.7 °C and with the data of Zhang et al.[26] for the swelling of bulk PMMA with CO_2 at 35 °C. Our swelling isotherms are significantly larger than those reported by Zhang et al. except at the lowest pressures (0−35 atm) where there is good agreement between our first sorption run isotherm and their swelling isotherm, which was reported as an average between the first desorption/second sorption runs. Our desorption isotherm is similar to the isotherm reported by Wissinger et al., which was measured on an unconditioned PMMA sample while increasing pressure, in the pressure range between 60 and 75 atm. However, our first sorption run isotherm is slightly lower than that reported by Wissinger et al. up to 60 atm but is larger at pressures higher than 75 atm.

To place the results for the anomalous maxima in perspective, a baseline may be constructed for each of the plots in the region where the anomalous maxima are observed in the swelling. An effective baseline is formed by interpolating the data on either side of the anomalous maxima as shown by the solid line in Figure

Table 1. CO_2 Adsorption and PMMA Swelling

temp (°C)	substrate	initial PMMA thickness (nm)	max excess thickness (nm)	press. at swelling max (atm)	menon correlation $P = P_c(T/T_c)^2$ (atm)	press. at max $(\partial\rho/\partial P)_T$ (atm)
35	SiO_2[a]	0	2.0	~73−76[b]	75	~79
35	SiO_2	88	2.5	~78−79	75	~79
35	SiO_2	321	16	~79	75	~79
35	GaAs	89	4.2	~78−79	75	~79
50	SiO_2	85		~100−113[c]	82	~101
50	SiO_2	325		~101−106[c]	82	~101

[a] Thermally grown SiO_2. [b] Pressure where adsorption maximum occurs. [c] Pressure corresponds to minimum in refractive index.

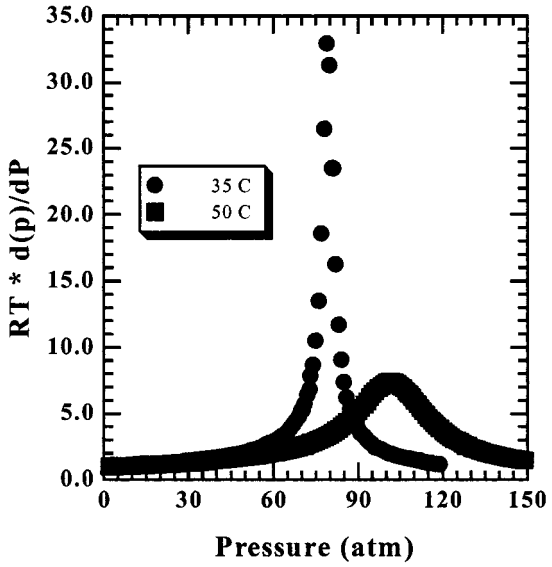

Figure 10. $(\partial\rho/\partial P)_T RT$ of CO_2 vs CO_2 pressure.

4. An effective excess thickness for sorption may be defined by taking the difference between the actual thickness and baseline for the swelling data. The maximum values of the effective excess thickness are listed in Table 1. The excess thickness increases from the case of adsorption of CO_2 on the bare SiO_2 surface to the swollen 88−89 nm PMMA films coated on both SiO_2 and GaAs. It further increases for the swollen 321 nm PMMA film on SiO_2.

Discussion

There are several factors that may produce the maxima in the swelling isotherms and the corresponding minima in the refractive indices in Figures 2−5. The swelling maxima occur in the regions of pressure/temperature where CO_2 exhibits a maximum in compressibility, i.e., where $(\partial\rho/\partial P)_T$ exhibits a maximum, as is evident upon comparison of the swelling data with the isothermal compressibility of pure CO_2 shown in Figure 10. The changes in compressibility with pressure at 35 °C are very sharp and larger in magnitude than the changes at 50 °C. The maximum in compressibility shifts to higher pressures as the temperature increases.[27] The same trend is observed in the anomalous swelling maxima.

Others have seen large adsorption excesses of compressible fluids onto hard impenetrable surfaces when operating in the proximity of the critical pressure and temperature.[10,12] For example, Findenegg observed large surface excesses of ethylene on graphitized carbon black surfaces.[10,28] At supercritical temperatures, the excess adsorption of ethylene exhibited a pronounced maximum at a pressure slightly less than the pressure where the compressibility of ethylene displayed a maximum. The excess adsorption isotherms were very large and sharp at near critical pressures and at temperatures that were slightly higher than the critical temperature. At higher temperatures the excess adsorption maxima become smaller and much broader in nature, occurring at higher pressures. Others have seen similar behavior in the supercritical adsorption of CO_2 on both unmodified and chemically modified silica surfaces as well as on proteins and polysaccharides.[11,12,29,30] Furthermore, da Rocha et al. showed that the excess adsorption of CO_2 at the CO_2−water interface leads to a minimum in the interfacial tension vs pressure at near-critical temperatures.[31] Several theoretical studies have also probed the supercritical adsorption of fluids on various surfaces.[8,14,32]

The surface excess of CO_2, Γ^{ex}, is given by

$$\Gamma^{ex} \equiv \int_{z_0}^{\infty} (\rho(z) - \rho_{bulk})\, dz \qquad (3)$$

where $\rho(z)$ is the local density of CO_2 at a distance z from the substrate, ρ_{bulk} is the density of the bulk CO_2, and z_0 represents the substrate surface. For many surfaces, the interaction between CO_2 and the surface may be expected to exceed the intermolecular attraction between pure CO_2 molecules, due to the low polarizability per volume of CO_2. Since CO_2 is attracted preferentially to the surface, $\rho(z)$ will be larger than ρ_{bulk}. In highly CO_2 compressible regimes, the attraction of CO_2 to the surface can produce $\rho(z)$ values with densities approaching those of liquid CO_2. The pronounced difference between $\rho(z)$ and ρ_{bulk} results in large excesses of CO_2 at the surface. As the pressure increases, the bulk density of CO_2 increases markedly, and the excess layer decreases since $\rho(z)$ becomes more equivalent to ρ_{bulk}. Thus, the qualitative behavior of Γ^{ex} should exhibit similar trends as that of the isothermal compressibility. For example, near the critical temperature large and sharp excess adsorption maxima are observed near the critical pressure. At higher temperatures, the maxima are smaller and broader and shift to higher pressures.

It is clear from Figure 8 that our measurements of thickness are sensitive to the adsorption of CO_2 onto the surface of SiO_2 in the compressible regime. This sensitivity arises because there is sufficient contrast in refractive index between the adsorbed CO_2 layer and the bulk CO_2. Good fits of the ellipsometric data are obtained by using the model in Figure 1a, assuming the refractive index of the adsorbed CO_2 layer is equivalent to that of a hypothetical liquid at 35 °C. The accurate fits of the model are consistent with the concept of a sharp interface between the adsorbed CO_2 layer and the SiO_2 substrate.

However, attempts to model an adsorbed CO_2 layer on the swollen PMMA films caused correlations and large statistical uncertainties in the fitting parameters.

Typically, these fits were inferior to those that were determined by assuming a single swollen polymer film. Another strategy that was employed was to fix the thickness of the swollen film at the baseline thickness given in Figure 4 and fit for the refractive index of the swollen polymer and the thickness of an adsorbed CO_2 layer. In these fits, an adsorbed CO_2 thickness could be extracted; however, the refractive indices of the swollen polymer films did not change much from those extracted assuming a single swollen polymer film. Also, the mean-square error on these fits were higher than the corresponding fits assuming a single polymer layer. The best fits were always achieved by assuming a single swollen polymer film. In contrast, the adsorbed CO_2 on the impenetrable SiO_2 surface exhibited a sharp interface according to the fits of the models.

A second observation suggests that the anomalous maxima in Figures 2−5 are not caused exclusively by an excess CO_2 wetting layer on the top of the polymer films. If the maxima were solely caused by such a CO_2 layer, then the anomalous peaks should become smaller as the thickness of the film increases, since the apparent swelling due to the wetting layer would be expected to become a smaller fraction of the total swelling. However, in Figures 3 and 4, the size of anomalous maxima did not change when increasing the initial thickness of the films by a factor of 3−4, suggesting that the anomalous swelling is not caused solely by a wetting layer on top of the polymer film. A similar way to rule out the concept of a surface-wetting layer only on top of the polymer film is to examine the effective excess thickness in Table 1. Notice that this excess thickness increases significantly as the initial film thickness increases from 88 to 321 nm. It would not have changed if the surface-wetting layer were only on top of the polymer film.

The substrate/polymer interactions can be varied by changing the substrate from SiO_2 to a less hydrophilic GaAs substrate. SiO_2 has surface silanol groups that can donate hydrogen bonds to PMMA, whereas GaAs lacks a stable oxide and thus cannot donate hydrogen bonds. The effect of the substrate/polymer interface interactions on the anomalous peaks for PMMA films is negligible when changing the substrate from SiO_2 to GaAs, as shown in Figure 4. Thus, the interactions at the substrate/polymer interface are not likely to be the cause of the anomalous swelling.

Finally, the swelling maxima cannot be attributed to sorption in the bulk film. Numerous swelling studies of *bulk* PMMA films do not exhibit a swelling maximum,[25,26] as seen in Figure 9. Clearly some other explanation is required to explain the anomalous maxima.

The discussion above suggests that the anomalous maxima are not caused by a single one of the following: a wetting layer on top of the polymer, sorption in the bulk film, or CO_2 interactions with the inorganic substrate. Therefore, we propose the swelling maxima arise from inhomogeneities in concentration at the free surface of the polymer extending to the substrate. As the compressibility of the solvent increases, the opportunity for large concentration inhomogeneities increases, as has been observed in simulations of grafted chains on surfaces.[8] As noted above, the excess thickness increases as the film thickness increases from 88 to 321 nm and then disappears for bulk films. Therefore, the anomalous peaks could be caused by surface excess properties over a distance greater than 100 nm. These large distances are characteristic of a surface excess layer that is diffuse at the polymer free surface. This observation of a diffuse surface layer is consistent with the failure of a model with sharp polymer and CO_2 layers to fit the data. In a bulk film, these composition inhomogeneities will also produce an effective excess thickness, but this excess thickness can be negligible compared with the large length change due to bulk swelling.

The inhomogeneities in concentration may be considered to be the onset of phase separation of CO_2 from the polymer film in the compressible regime. The effects of compressibility on stability and bulk phase separation may be described with macroscopic thermodynamics. In general, a bulk binary mixture is stable if it satisfies the following condition[33]

$$g_{xx} \equiv \left(\frac{\partial^2 g}{\partial x^2}\right)_{T,P} > 0 \tag{4}$$

where g is the intensive Gibbs free energy per mole, per mass, etc., and x is any concentration variable. Now, g_{xx} can be further separated into compressible and incompressible components

$$g_{xx} = a_{xx} - \nu\kappa P_x^{\,2} \tag{5}$$

where a is the intensive Helmholtz free energy, ν is the intensive volume, and κ is the isothermal compressibility. Furthermore

$$a_{xx} = \left(\frac{\partial^2 a}{\partial x^2}\right)_{T,\upsilon} \tag{6}$$

$$\kappa = -\left(\frac{\partial \ln \upsilon}{\partial P}\right)_{T,x} \tag{7}$$

$$P_x = \left(\frac{\partial P}{\partial x}\right)_{T,\upsilon} \tag{8}$$

In eq 5, a_{xx} represents the incompressible contribution to g_{xx}, and the negative $\nu\kappa P_x^2$ term represents the compressible contribution to g_{xx}. The compressible contribution to g_{xx} is unfavorable to phase stability, as this term is always negative. Thus, eq 6 shows that a compressible solution is always less stable than the corresponding incompressible solution.[33]

In our system at 35 °C, the compressibility of CO_2 displays a sharp maximum in compressibility in the same region of pressure that the maximum in swelling is observed. The solubility of CO_2 in the polymer film may be expected to decrease as the compressibility increases. This decrease in solubility may result in CO_2-rich and PMMA-rich domains within the polymer film. The ellipsometric measurements do not yield the domain size of the phase-separated regions. Thus, it was not meaningful to include composition gradients in the polymer film layer; this would only add adjustable parameters. The fact that the swelling does not decrease on the low-pressure side of the anomalous maxima with an increase in pressure suggests that the CO_2 does not leave the polymer film. Instead, the phase-separated CO_2, with a larger molar volume than the partial molar volume of the dissolved CO_2, is distributed throughout the film and lowers the measured refractive index. This explanation is consistent with the large decrease in the refractive index of the film in the anomalous pressure

region. As the pressure is further increased, the compressibility of CO_2 decreases and CO_2 becomes more soluble, and hence denser within the polymer film, resulting in a decrease in the polymer swelling and an increase in the refractive index.

The phenomenon that is observed, i.e., the thickening of the thin film and the drastic reduction in refractive index, is consistent with inhomogeneities in concentration, essentially the onset of phase separation in the film. The film would expand (a foaming action) to accommodate the low-density CO_2 regions that would develop in the film. The fact that the CO_2 is not expelled from the film with a concomitant reduction in film thickness over the experimental time scales suggests the CO_2-rich domains are quite small relative to the film thickness. It is further speculated that there is some interplay or coupling of the bulk phase separation process with the critical wetting phenomena on the film surface that allows the CO_2 to remain and to expand the film. This concept is supported by the fact that CO_2 films may remain on hard surfaces without evaporating. Overall, this mechanism is consistent with the shape of the anomalous peaks and the insensitivity in the swelling isotherms to film thickness or substrate interactions. It is also consistent with the temperature dependence of the size and location of the anomalous maxima, in that they follow the behavior of the isothermal compressibility.

At 35 °C, the pressure corresponding to the maxima in the PMMA swelling was slightly larger than the pressure where the adsorption maximum occurred on the pure SiO_2 substrate. These subtle changes in pressure are important as small changes in pressure produce large changes in CO_2 activity and density in the near-critical region. As seen in Table 1, the maximum pressure for the CO_2 adsorption on bare SiO_2 at 35 °C agrees well with Menon's correlation.[34] Menon found good agreement with the following empirical equation, which is based on Polanyi's potential theory of adsorption for gases, for determining the pressure at which maximum excess adsorption occurs for various macroporous adsorbent−adsorbate systems[34,35]

$$P_{max} = P_c\left(\frac{T}{T_c}\right)^2 \tag{9}$$

where P_{max} is the pressure where the maximum excess adsorption occurs, T is the temperature, and P_c and T_c are the critical pressure and critical temperature, respectively. In contrast, the pressures at which the maxima occur in the swelling isotherms and corresponding minima occur in the refractive indices agree well with the pressure at which the compressibility, or similarly $(\partial\rho/\partial P)_T$, exhibits a maximum. The higher pressure required with the PMMA film may reflect the different interactions between the CO_2−SiO_2 and the CO_2−PMMA systems. It may also reflect different mechanisms involved for penetration of CO_2 into the soft polymer film vs adsorption on the hard substrate surface.

Conclusion

Spectroscopic ellipsometry was used successfully to measure the swelling of thin films of PMMA coated on both SiO_2 and GaAs. At 35 and 50 °C, the swelling reaches a value of ∼21% at the highest pressures studied (100−135 atm). Anomalous maxima in the swelling isotherms and corresponding minima in the refractive indices are observed in the regions of pressure where the compressibility of CO_2 becomes large. These maxima in the swelling isotherms have not been observed in the swelling of bulk films. The maxima/minima are large and sharp at 35 °C and smaller and broader at higher pressures at 50 °C, much like the behavior of the isothermal compressibility of pure CO_2. The swelling maxima are insensitive to changing the substrate from silicon to GaAs. In addition, an effective excess thickness due to the anomalous swelling maxima increases proportionally with increasing initial film thickness for the range studied of 85 nm < h_0 < 325 nm. The anomalous maxima are consistent with inhomogeneities in concentration at the free surface of the polymer extending to the substrate, essentially the onset of phase separation (foaming) driven by the increased compressibility of the system. This mechanism is consistent with the size, shape, and temperature dependence of the swelling maxima as well as the insensitivity of the percent swelling to initial film thickness or substrate interactions.

Large surface excesses of CO_2 are also seen on a bare SiO_2 wafer due to surface adsorption of CO_2. The pressure at which the maximum thickness of adsorbed CO_2 occurs is lower than the pressure where the maxima in the swelling isotherms occur. The higher pressure required with the PMMA film may reflect the different interactions between the CO_2−SiO_2 and the CO_2−PMMA systems as well as the different mechanisms involved for the sorption of CO_2 into the soft polymer film vs adsorption on the hard substrate surface.

The swelling isotherms show dual-mode behavior, indicative of the glassy state, at the lowest CO_2 pressures. Thus, solvent-induced glass transitions can be extracted from the ellipsometric measurements through the onset of hysteresis between the initial swelling isotherms and the subsequent desorption swelling isotherms. The CO_2-induced glass transitions agree with previous measurements.[36]

Acknowledgment. This work is supported by the Department of Energy and the National Science Foundation (DMR-0072898).

References and Notes

(1) Cooper, A. I. *J. Mater. Chem.* **2000**, *10*, 207−234.
(2) Kazarian, S. G. *Appl. Spectrosc. Rev.* **1997**, *32*, 301−348.
(3) Goel, S. K.; Beckman, E. J. *AlChE J.* **1995**, *41*, 357−367.
(4) Taylor, D. K.; Carbonell, R.; DeSimone, J. M. *Annu. Rev. Energy Environ.* **2000**, *25*, 115−146.
(5) Gabor, A. H.; Allen, R. D.; Gallagher-Wetmore, P.; Ober, C. K. *Proc. SPIE−Int. Soc. Opt. Eng.* **1996**, *2724*, 410−417.
(6) Watkins, J. J.; McCarthy, T. J. *Chem. Mater.* **1995**, *7*.
(7) Goldfarb, D. L.; de Pablo, J. J.; Nealey, P. F.; Simons, J. P.; Moreau, W. M.; Angelopoulos, M. *J. Vac. Sci. Technol. B* **2000**, *18*, 3313−3317.
(8) Meredith, J. C.; Sanchez, I. C.; Johnston, K. P.; Pablo, J. J. *J. Chem. Phys.* **1998**, *109*, 6424−6434.
(9) Meredith, J. C.; Johnston, K. P. *Langmuir* **1999**, *15*, 8037−8044.
(10) Findenegg, G. H. In *Fundamentals of Adsorption*; Myers, A. L., Belfort, G., Eds.; Engineering Foundation: New York, 1984.
(11) Strubinger, J. R.; Parcher, J. F. *Anal. Chem.* **1989**, *61*, 951−955.
(12) Strubinger, J. R.; Song, H.; Parcher, J. F. *Anal. Chem.* **1991**, *63*, 98−103.
(13) Sirard, S. M.; Green, P. F.; Johnston, K. P. *J. Phys. Chem. B* **2001**, *105*, 766−772.

(14) Rangarajan, B.; Lira, C. T.; Subramanian, R. *AIChE J.* **1995**, *41*, 838−845.
(15) Keddie, J. L.; Jones, R.; Cory, R. *Faraday Discuss.* **1994**, *98*, 219−230.
(16) Tiberg, F.; Jonsson, B.; Tang, J.; Lindman, B. *Langmuir* **1994**, *10*, 2294−2300.
(17) Papanu, J. S.; Hess, D. W.; Bell, A. T.; Soane, D. S. *J. Electrochem. Soc.* **1989**, *136*, 1195−1200.
(18) Cras, J. J.; Rowe-Taitt, C. A.; Nivens, D. A.; Ligler, F. S. *Biosens. Bioelectron.* **1999**, *14*, 683−688.
(19) Herzinger, C. M.; Johs, B.; McGahan, W. A.; Woollam, J. A.; Paulson, W. *J. Appl. Phys.* **1998**, *83*, 3323−3336.
(20) Obriot, J.; Ge, J.; Bose, T. K.; St-Arnaud, J. M. *Fluid Phase Equilib.* **1993**, *86*, 315−350.
(21) Philipp, H. R. In *Handbook of Optical Constants of Solids*; Palik, E. D., Ed.; Harcourt Brace Javanovich: Orlando, 1985; Vol. 1.
(22) Jellison, G. E. *Opt. Mater.* **1992**, *1*, 41.
(23) Michels, A.; Hamers, J. *Physica IV* **1937**, 995−1006.
(24) Tompkins, H. G.; McGahan, W. A. *Spectroscopic Ellipsometry and Reflectometry*; John Wiley & Sons: New York, 1999.
(25) Wissinger, R. G.; Paulaitis, M. E. *J. Polym. Sci., Part B: Polym. Phys.* **1987**, *25*, 2497−2510.
(26) Zhang, Y.; Gangwani, K. K.; Lemert, R. M. *J. Supercrit. Fluids* **1997**, *11*, 115−134.
(27) Levelt Sengers, J. M. H. In *Supercritical Fluid Technology*; Bruno, T. J., Ely, J. F., Eds.; CRC Press: Boca Raton, FL, 1991.
(28) Specovius, J.; Findenegg, G. H. *Ber. Bunsen-Ges. Phys. Chem.* **1980**, *84*, 690−696.
(29) Hoshino, T.; Nakamura, K.; Suzuki, Y. *Biosci. Biotechnol. Biochem.* **1993**, *57*, 1670−1673.
(30) Nakamura, K.; Hoshino, T.; Ariyama, H. *Agric. Biol. Chem.* **1991**, *55*, 2341−2347.
(31) da Rocha, S. R. P.; Harrison, K. L.; Johnston, K. P. *Langmuir* **1999**, *15*, 419−428.
(32) Tan, Z.; Gubbins, K. E. *J. Phys. Chem.* **1990**, *94*, 6061−6069.
(33) Sanchez, I. C.; Stone, M. T. In *Polymer Blends*; Paul, D. R., Bucknall, C. B., Eds.; John Wiley & Sons: New York, 2000; Vol. 1.
(34) Menon, P. G. *J. Phys. Chem.* **1968**, *72*, 2695−2696.
(35) Dubinin, M. M. *Chem. Rev.* **1960**, *60*, 235−241.
(36) Condo, P. D.; Johnston, K. P. *J. Polym. Sci., Part B: Polym. Phys.* **1994**, *32*, 523−533.

MA011384W